
STRUCTURE, PHASE TRANSFORMATIONS,
AND DIFFUSION

Explosive Welding: Mixing of Metals without Mutual Solubility (Iron–Silver)

B. A. Greenberg^a, M. A. Ivanov^b, V. V. Rybin^c, O. A. Elkina^a, A. V. Inozemtsev^a,
A. Yu. Volkova^a, S. V. Kuz'min^d, and V. I. Lysak^d

^a*Institute of Metal Physics, Ural Branch, Russian Academy of Sciences, ul. S. Kovalevskoi 18, Ekaterinburg, 620990 Russia*

^b*Kurdyumov Institute of Metal Physics, National Academy of Sciences of Ukraine, bul'v. Vernadskogo 36, Kiev, 03680 Ukraine*

^c*State Polytechnical University, ul. Politekhnicheskaya 29, St. Petersburg, 195251 Russia*

^d*State Technical University, pr. Lenina 28, Volgograd, 400131 Russia*

Received March 6, 2012;
in final form April 4, 2012

Abstract—The results obtained for joints of dissimilar metals, iron–silver (earlier, copper–tantalum), which form immiscible liquid suspensions, explain why they are mixed in explosive welding. Inhomogeneities of the wavy interface, such as protrusions and zones of localized melting, were observed. The effect of granulating fragmentation, which is responsible for crushing initial materials into particles, was understood as one of the most efficient ways to dissipate the supplied energy. It is shown that, in the case of joints of metals without mutual solubility, zones of localized melting represent colloidal solutions, which form either emulsions or suspensions. At solidification, the emulsion represents a hazard for joint stability due to possible separation; on the contrary, suspension can enable the dispersion strengthening of the joint. The results can be used in the development of new metal joints without mutual solubility.

Keywords: explosive welding, mutual solubility, mixing, melting, fragmentation, colloidal solution

DOI: 10.1134/S0031918X12110075

INTRODUCTION

Explosive welding is a very swift process and has little similarity to other methods of joining materials. It seems outwardly simple; however, it is very complex in its physical nature; this process requires not only a detailed structural analysis, but also a new approach. With all of the variety of materials and welding regimes, the central problem is intermixing in the transition zone near the interface [1, 2]. Mixing occurs as a result of a strong external impact, which presumes large plastic deformation (including pressure, shear components, rotating moments of the stress, strain inhomogeneity, etc.), surface friction, the cumulative jet effect, and other factors. However, it has so far remained unclear how, in such a short welding time, the metals have time to mix, even at such strong external action. This question is most urgent when considering materials that have no mutual solubility.

The existence of a so-called “window of weldability” (defined in coordinates as the collision angle vs. the velocity of motion of the contact point) is the necessary condition for the formation of a firm joint. To identify the main processes that determine weldability, the structure of joints must be studied. Currently, however, the role of structural studies is underestimated and, in general, they are limited to optical microscopy. In this work, optical (OM), scanning (SEM), and

transmission electron (TEM) microscopy methods are used to study the structure of welded joints.

Previously, we investigated the welded joints of the metals (titanium–orthorhombic titanium aluminide) with normal mutual solubility in liquid and solid states [3–6]. VTI-1 and VTI-4 alloys have been selected as aluminides. Depending on the welding conditions, joints with the following various types of interfaces were obtained:

(A_w) titanium VTI-1, wavy interface;

(A_p) titanium VTI-1, flat interface, along which melting occurred;

(B_w) titanium VTI-4, wavy interface;

(B_p) titanium VTI-4, nearly flat, partially molten interface.

In these joints, protrusions were detected for the first time as typical structural heterogeneities of the interface. In some joints, melting was observed along the whole interface, while in others, it was observed in the localized-melting zone with a vortex structure. In any case, the melts present true solutions, in which mixing occurs at the atomic level.

Next, for explosive welding, we selected copper and tantalum, which have no mutual solubility [7–9]. Welding was performed at Volgograd State Technical University. Two welding regimes were employed. Here, we present only the basic welding parameters for

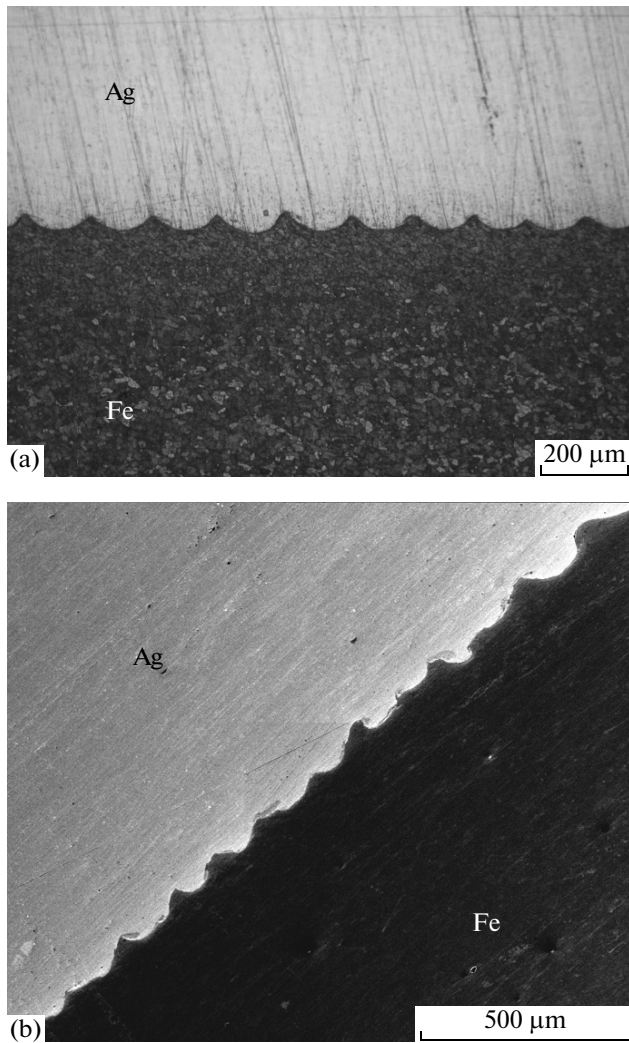


Fig. 1. Fe–Ag wavy interface (transverse section): (a) OM image and (b) SEM image.

further comparison, i.e., the collision angle γ ; the velocity of motion of the contact point V_{con} ; the velocity of collision V_{col} ; and the energy consumed in plastic deformation W_2 , as follows:

$(C_p) \gamma = 5.22^\circ$, $V_{\text{con}} = 2680$ m/s, $V_{\text{col}} = 234$ m/s, $W_2 = 0.33$ MJ/m²; flat interface.

$(C_w) \gamma = 11.8^\circ$, $V_{\text{con}} = 2125$ m/s, $V_{\text{col}} = 440$ m/s, $W_2 = 1.04$ MJ/m²; wavy interface.

The choice of parameters (C_p) corresponds to the lower limit of the weldability range, whereas the parameters (C_w) fall into the weldability window. In [7–9], different types of heterogeneities have been identified, as well as typical interfaces substantial for mixing in the absence of mutual solubility. Both similarities and differences were found in the structure of titanium–orthorhombic titanium aluminide (referred to be below, for brevity, as titanium–aluminide). It is also determined whether the localized-melting zones

are true solutions, as in the normal-solubility case, or if they have a different structure.

In this paper, which is a continuation of [9], the area of the investigation of metal joints that have almost no mutual solubility has been extended by including an iron–silver pair. In both cases, these are pairs of dissimilar metals that differ greatly from each other with regard to their melting points and hardness. Pairs of these metals form immiscible liquid suspensions in the molten state. We will also try to answer why immiscible suspensions mix.

EXPERIMENTAL

Explosive welding was carried out using different schemes and parameters at Volgograd State Technical University. We selected the joints to be studied based on the obtained results. In the scheme we used, the parallel arrangement of the plates was employed. The immobile plate was located on a metallic substrate. Welding was performed at the following parameters:

$$(D_w) \gamma = 15.6^\circ, V_{\text{con}} = 1910 \text{ m/s}, V_{\text{col}} = 520 \text{ m/s}, \\ W_2 = 0.73 \text{ MJ/m}^2.$$

The Armco iron plate was 1.5 mm thick, while the silver plate was 2 mm thick.

The metallographic analysis was carried out using an Epiquant optical microscope equipped with a SIAMS computing system. The study of the microstructure was conducted using JEM 200CX and SM-30 Super Twin transmission electron microscopes, Quanta 200 3D.

EXPERIMENTAL RESULTS

As mentioned above, in the previously studied copper–tantalum joint, both flat and wavy boundaries were observed in different regimes of explosive welding. Figure 1 shows OM and SEM images of the iron–silver interface. The wavy shape of the boundary is fairly regular (Fig. 1a), though it contains waves of different amplitudes and even almost straight sections (Fig. 1b). The average wavelength is about 140–150 μm and the amplitude is about 50 μm . SEM images are presented below without “SEM” indications in the figure captions.

In the case of a wavy boundary, the interface is corrugated so that its longitudinal section exhibits a set of alternating bands of iron and silver with parallel boundaries. The SEM image in Fig. 2 was taken from the inclined section, rather than the longitudinal section (white bands are silver). Therefore, only a few bands are seen and protrusions are observed at the interface. Even if the wavelength and amplitude of the wave surface change, the surface remains smooth. However, if there is a protrusion (as a cone with a sharp or smoothed apex), the surface is no longer smooth. The size of protrusions is dozens of microns; in some cases, it reaches 100 μm . As numerous SEM content

measurements have shown, these protrusions are iron. Protrusions were observed for the first time in [4] in a titanium–aluminide joint, then in [7] in a copper–tantalum joint.

As can be seen from Fig. 2a, the bands can become broken or branched, or be divided into parts. Some areas exhibit an interface that lost its wavy character. Zones of local melting (darker than adjacent bands of silver) are already visible in Fig. 2a and, at a larger magnification, in Fig. 2b. These zones are clearly visible in Fig. 2c, i.e., dark iron particles against a silver background.

Data on the chemical composition of the localized-melting zones (Figs. 3a, 3b) are obtained by means of SEM using multiple measurements. Figure 3 displays the regions where measurements had been made. Figure 3b clearly shows iron particles against the silver background. The table lists the concentrations of elements. As can be seen from the table, the chemical composition in the center of zones is approximately 60Ag–40Fe (at %). The structure composition observed in the zone indicates the penetration of elements of one material into another.

The internal structures of the localized-melting zones are shown in Fig. 4. In Fig. 4a, the arrow marks the region whose structure is shown in Fig. 4b at higher magnification. A similar structure can also be seen in Figs. 4c, 4d. As suggested by Figs. 4b and 4d, spherulites are formed during the solidification of molten silver; however, ultra-rapid quenching and many nuclei with slow growth also occur. The density of spherulites turned out to be less in Fig. 4d, so they can be seen. One should note their quite perfect spherical shape, which minimizes the surface energy. Spherulites have dimensions of 100–200 nm. Figures 4b and 4d clearly illustrate that the concentration of iron particles is much smaller (about one order of magnitude) than that of silver particles. At first glance, this contradicts the results listed in the table. However, this is a spurious contradiction. Thus, Fig. 3b already shows that the structure of the localized-melting zone is heterogeneous; there are almost no visible particles of iron below square no. 5. Moreover, it follows from the simultaneous existence of concentrated and unconcentrated solutions that, due to ultrafast quenching, the separation of the concentrated solution may be unlikely.

Previously, among the various titanium–aluminide joints (different compositions of aluminide and at different regimes), spherulites were only observed in an (A_p) joint between titanium and VTI-1 alloy, and only if the flat interface was molten [4]. Figure 4e shows the SEM image of the structure of such an interface that contains spherulites. Compared to Fig. 4d, one can see that the sizes of titanium spherulites (200–400 nm) are greater than those of silver spherulites. As illustrated in Fig. 4f, in the case of the (C_p) copper–tantalum joint, the zone of localized melting has a different structure;

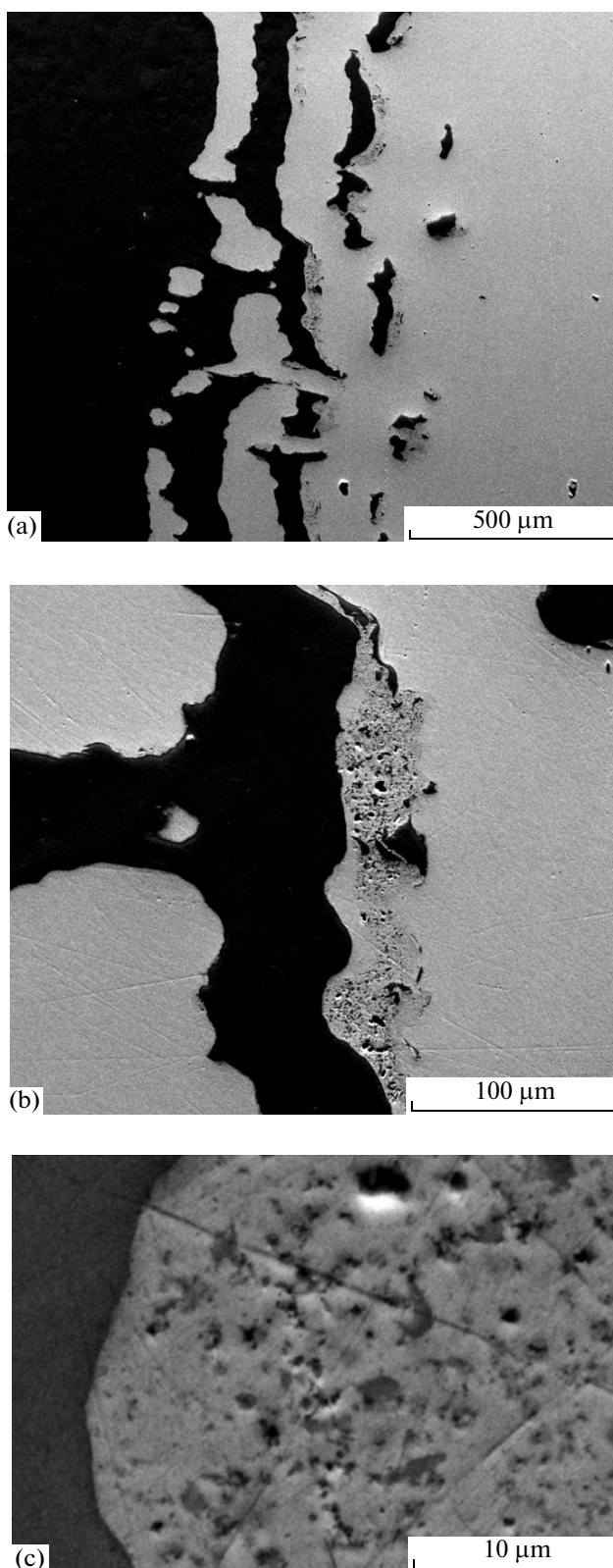


Fig. 2. Inhomogeneities of interface (longitudinal section): (a) protrusions; (b, c) zones of localized melting (at various magnifications).

Results of spot measurements of chemical composition of zone of localized melting

Measurement no.	Content Ag, at %	Content Fe, at %
1	97	3
2	97	3
3	0	100
4	56	44
5	62	38
6	100	0
7	2	98

no spherulites are observed and the concentration of both phases are similar.

In the case of the iron–silver joint, the zone of localized melting presents silver containing fragments of iron. Here, vortices could be formed, similar to those observed in titanium–titanium aluminide joints [3, 5]. However, no vortices were observed here, possibly due to the fact that the melt contained solid particles, which efficiently increased its viscosity.

Figure 5 shows multiple protrusions and, as chemical analysis evidences, a lot of silver particles within the band of iron. Here, in addition, the dendrites are visible within a band of silver, which will be considered in detail below.

Some of the features mentioned of the interface are more clearly visible in the relief SEM image taken after the iron was completely etched away (Fig. 6).

This image displays silver ridges instead of bands, which are broken lines. There are also visible necks between the ridges, which significantly distorts the interface. The breaks observed in the alternation of bands in the longitudinal section, including the loss of continuity, reflect the imperfection of this interface. Figure 7 shows the TEM image of a localized-melting zone. Black voids are left by the particles of iron after they were etched. Judging from the observed voids, iron particles had arbitrary shapes. The electron diffraction pattern shows only the presence of silver.

As mentioned above, a region of silver filled with dendrites arises near the iron–silver interface, which are known to be evidence of melting. As can be seen from Fig. 8a (transverse section), this region stretches along the entire interface, including areas of local melting. The width of the region (vertically from the interface) is approximately 200–250 μm . In the longitudinal section (Fig. 8b), there are visible single dendrites with both primary and secondary branches. Silver particles are also clearly visible within the iron band, as discussed above. Figure 8b demonstrates both dendrites and a fine-crystalline interdendritic area. Referring to Fig. 3a, note that the entire measuring region no. 1 is composed of close packed dendrites with some dendrites growing into the adjacent area of silver that avoided melting.

In the case of copper–tantalum, no dendrites were observed. Among the various titanium–aluminide joints, dendrites were only observed in (B_p) titanium–VTI-4 alloy in the regime when the almost flat interface was partially molten. Figure 8d shows an SEM

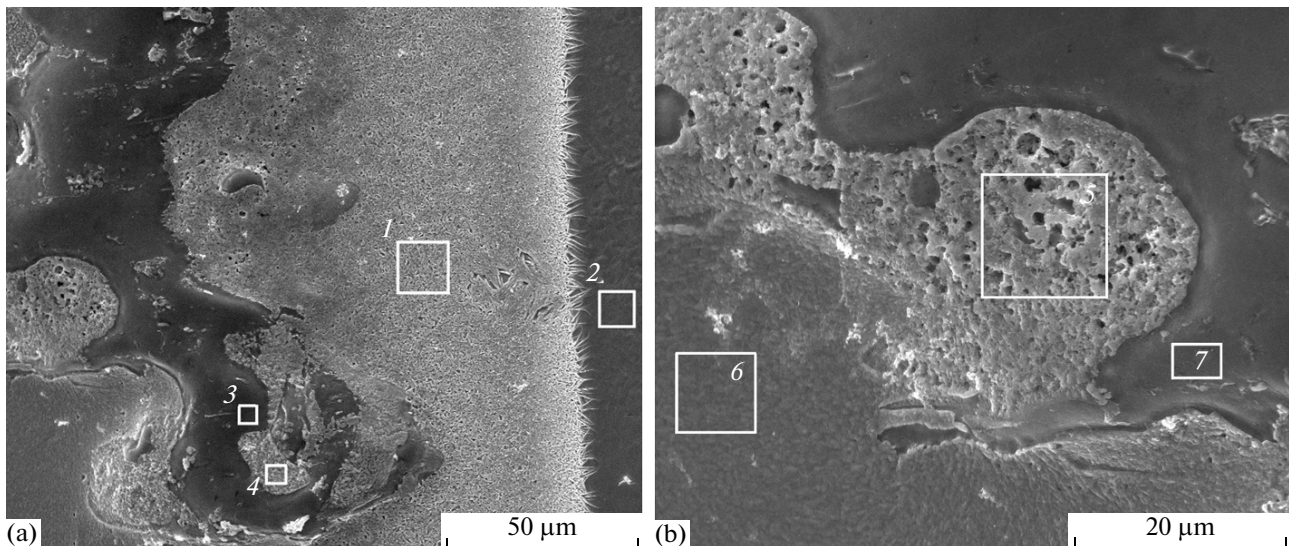
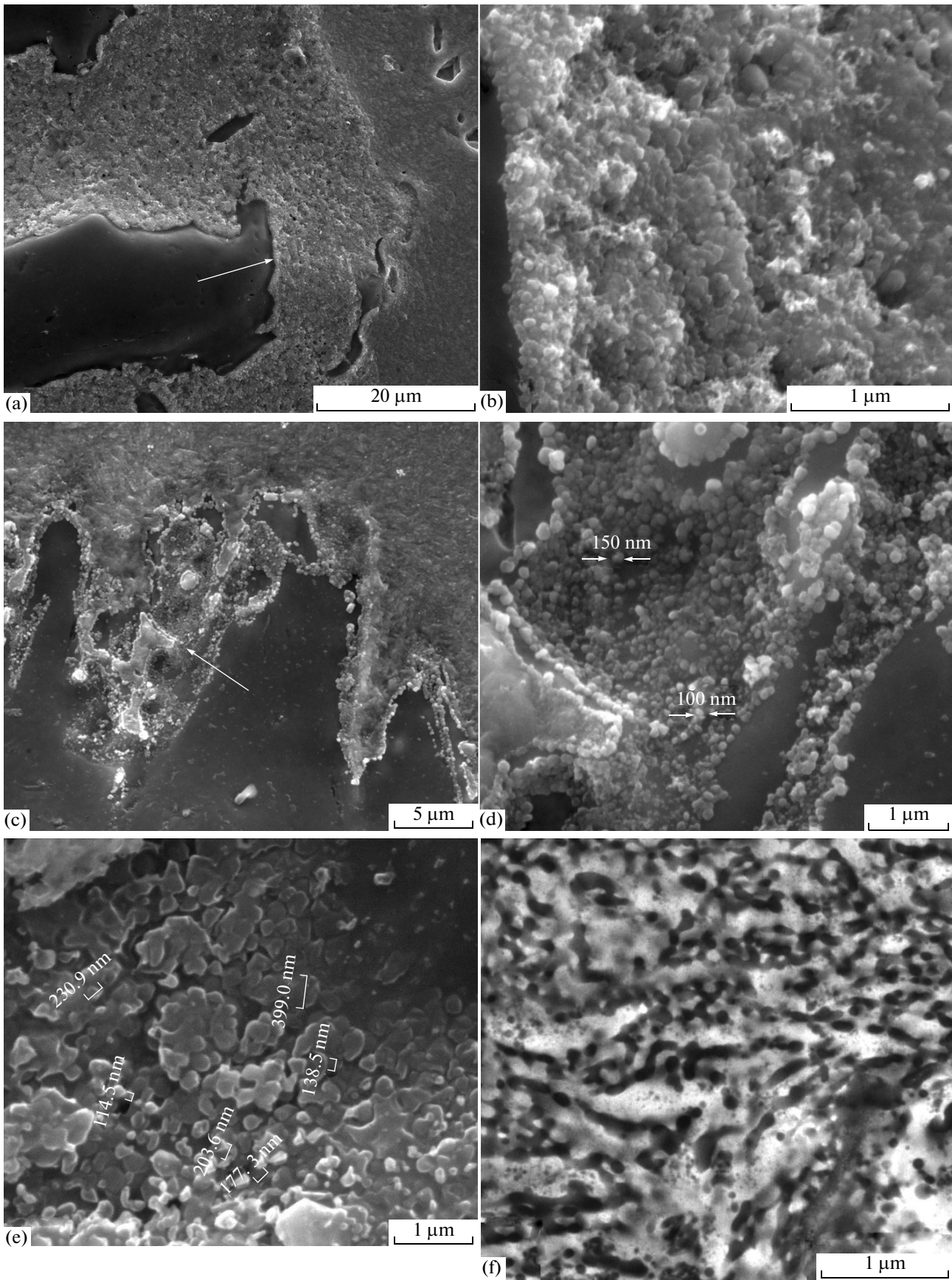


Fig. 3. Zones of localized melting (longitudinal section): (a) near interface and (b) internal zone structure; points of measurements are indicated.

Fig. 4. Zones of localized melting (longitudinal section) in (a)–(d) Fe–Ag, (e) Ti–VTI-1, and (f) Cu–Ta: (a), (c) at low magnification; (b, d) at high magnification; silver spherulites; (e) titanium spherulites, and (f) particles of copper and tantalum.



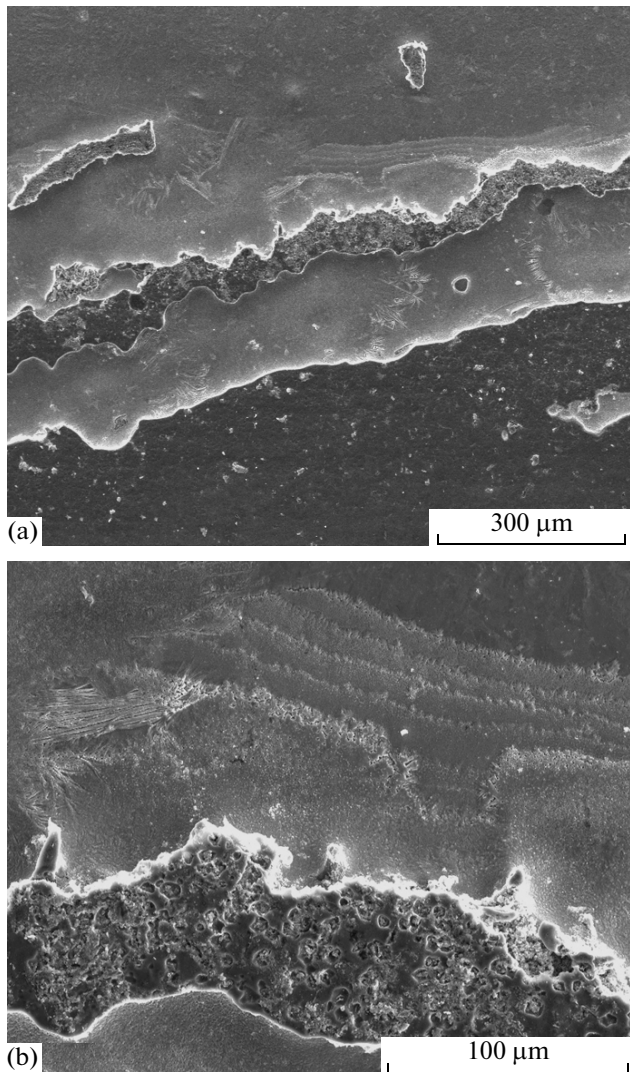


Fig. 5. Iron bands containing silver particles (longitudinal section): (a, b) various magnifications; dendrites are visible.

image of the structure of this region containing titanium dendrites.

Figure 9 exhibits (a) a cellular, (b) a band, and (c) recrystallized structures of silver that are typical of severe deformation. We consider that these structures correspond to the solid undergone no melting. Similar structures have been observed previously in the titanium–aluminide [3] (Fig. 8) and copper–tantalum [7] (Fig. 10) joints.

In this paper, the microhardness was measured at various points in the transition zone. It was found that the microhardness (about 750 MPa) in the region of the local melting of silver containing iron particles exceeds the minimum microhardness obtained in the silver region with a dendritic structure (approximately 450 MPa). However, this excess is far less than that observed previously in the case of the localized-melt-

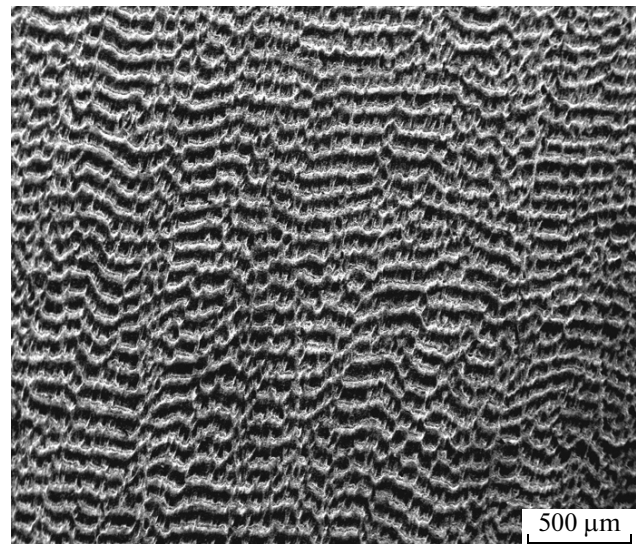


Fig. 6. Longitudinal section of the transition zone (iron etched): ridges of silver are visible.

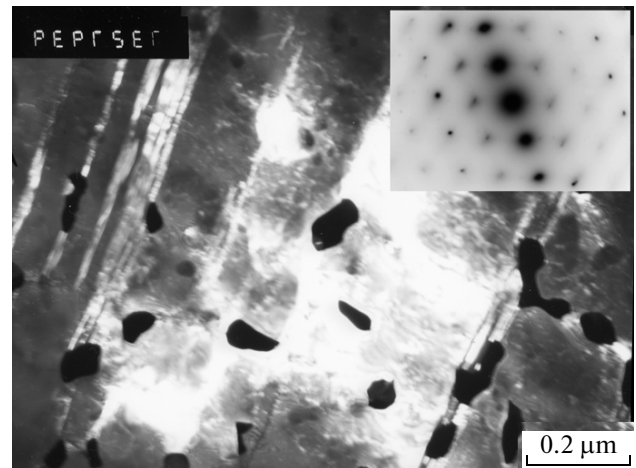


Fig. 7. TEM dark-field image in the reflection $\langle 111 \rangle_{Ag}$ of the zone of localized melting (iron etched): voids left by iron particles are visible.

ing zones of copper with tantalum particles (see [7], Fig. 13). In this case, the microhardness in the zone of localized melting is 4000 MPa, which is 3000 MPa greater than the microhardness of copper. It can be assumed that stronger precipitation hardening observed in the case of copper–tantalum is primarily due to the greater hardness of tantalum compared to iron and, secondarily, the higher concentration of tantalum particles compared to iron particles.

DISCUSSION

Inhomogeneities of the Interface

Throughout this paper, we focused on the imperfection of the wavy iron–silver interface. If one restores the interface using the observed sections, numerous distortions in and deviations from the ideal

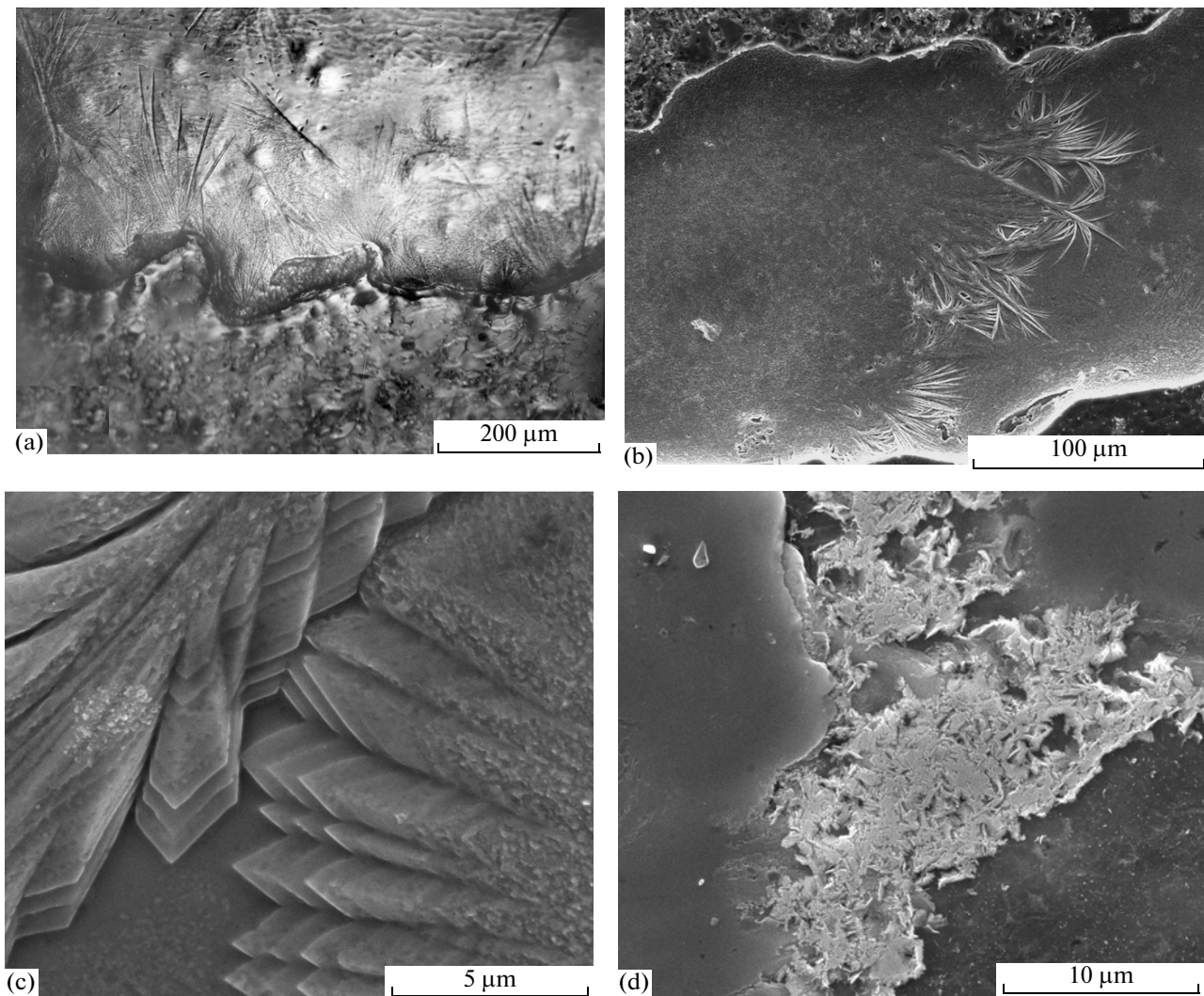


Fig. 8. Areas of (a–c) silver and (d) titanium filled with dendrites: (a) transverse section (OM); (b), (c) longitudinal section (SEM) at different magnifications; (b) silver particles within the iron band; (c) fine-crystalline interdendritic region; (d) longitudinal section for (B_p) titanium–VTI-4 joint.

periodic form will be found, regardless of the size of the protrusion, which is a key factor that determines the heterogeneity of the wavy interface. Due to the presence of protrusions, regions filled with any welding materials can be found on each side near the interface, which indicates their interpenetration. The formation of protrusions does not depend on the mutual solubility of the initial metals. Protrusions were observed in all the joints we have examined and for both flat and wavy interfaces. Protrusions are formed by the harder metal in the pair, i.e., aluminide, tantalum, or iron. A key point is the formation of protrusions at the flat interface (C_p , a copper–tantalum joint). Only the formation of protrusions can explain the observation, in this case, of three types of regions filled with either the original metal or a mixture thereof.

If the interface is smooth it creates problems with bonding between metals of the pair, which would

require either the reconstruction of metallic chemical bonds, or provide the transport of point defects. However, the presence of protrusions solves the problem of surface bonding; the protrusions play the role of nails. Another process that affects bonding is the local melting of the metals near the interface. As has been shown in this and previous studies [3–9], the internal structure of the localized-melting zones greatly depends on the mutual solubility of the metals. We believe that local melting is initiated by the granulating-type fragmentation.

Granulating Fragmentation

For all joints studied, including titanium–titanium aluminide, copper–tantalum, and iron–silver, we obtained electron microscopy images of different zones in which there are many particles of micron and

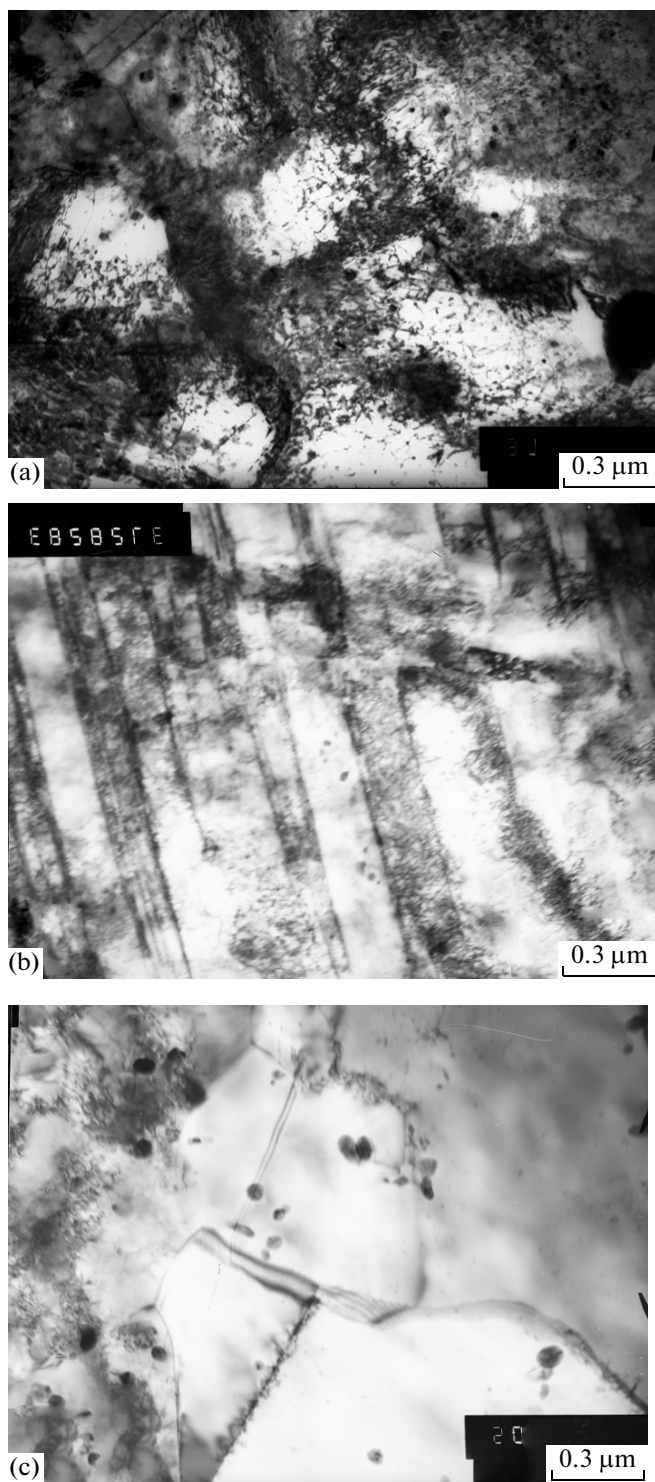


Fig. 9. Structure of highly deformed silver: (a) cellular, (b) band, and (c) recrystallized.

nanoscaled sizes. Fragmentation into particles occurs both with and without normal solubility, no matter what form the interface has, i.e., wavy or flat. In addition to the particles emitted from one material to another, continuous layers were observed that consist

of particles that interlock with each other, but insufficiently tightly. This layer has been found in titanium–titanium aluminide in [5], where Fig. 7 displays the SEM image of this layer formed by titanium aluminide. Moreover, Fig. 11 in [9] shows an SEM image of a fragmented layer of tantalum in copper–tantalum.

Then, the question of which way do the particles originate arises. Reasonable assumption is the fragmentation of material. The possibility of a special type of fragmentation is supposed, which we call the granulating fragmentation (GF). It is a fundamentally different type of fragmentation in comparison with the well-known fragmentation, whose existence has been confirmed by numerous observations of the structure of materials upon severe deformation [10]. The classical fragmentation involves piling up dislocations (and twins), as well as the formation of coiled, cellular, and band structures and recrystallization (see Fig. 9).

The above observation of silver particles within the iron bands is the result of the GF of silver, and the observation of iron particles in zones of localized melting is the result of the GF of iron. In [11], TEM observations on micron iron particles separations from the interface and their movement to a distance of 100 μm in a layer of aluminum are also given for the case of iron–aluminum joints.

The consideration of the possibility of two types of fragmentation is the basis for a new approach to describing welded joint structures. Both types of fragmentation are implemented at different distances from the interface; i.e., GF occurs near the interface, where the impact is greater, and classical fragmentation takes place a little further from the interface. In our opinion, GF proceeds for a time on the order of the impact time, i.e., GF is a much more rapid process than classical fragmentation. In the case of GF, the characteristic times are roughly estimated to be a microsecond and, in the case of the classical fragmentation, they are estimated to be 10^8 – 10^9 μs (the structural relaxation time).

Despite that the temperature in the contact area can be quite high the internal impact is so fleeting that the thermally activated processes that determine the movement and rearrangement of dislocations are not possible. It can be assumed that these processes, as well as diffusion, can only be possible due to the effect of residual stresses and temperature. These are processes that determine the classical fragmentation, whereas the GF occurs almost without the participation of dislocations. Under the rigid conditions that are implemented in explosive welding, including the lack of relaxation mechanisms of dislocations, one of the most efficient channels of energy dissipation is the formation of surfaces that have the maximum total area. These may include free surfaces, followed by destruction. These may be the surfaces resulting from microdestruction. It should be emphasized that all these processes are athermal and can happen almost instantaneously.

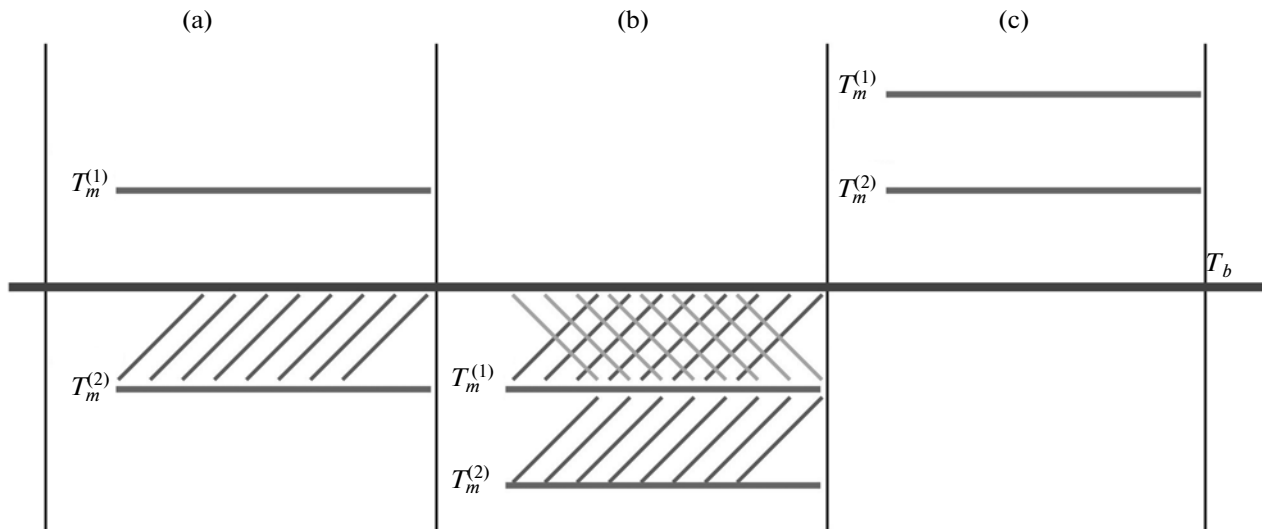


Fig. 10. Schematic representation of the various sequences of the characteristic temperatures.

GF is a process of separation into particles, which either fly apart or merge with each other. Possible ways of merging can be similar to those presented in [12]. To a certain extent, GF is analogous to fragmentation under explosion, which was studied by Mott [13]. In both cases, there occurs granulation and dispersion of the particles, but only in the case of GF, the continuity of materials is preserved because the dispersion of particles takes place in a confined space. GF is a powerful channel for the dissipation of the supplied energy, since the surface of the particles flying apart has a large total area, which is the main role of the GF. As an alternative process to destruction, GF increases the survivability of the material, which saves it from destruction, even under such a strong external impact as explosive welding.

Borders of the GF fragments, in our opinion, are incomplete, so that the connection between the fragments is weaker than between grains. This fact makes rotations and movement of the fragments possible. It can be expected that the processes of GF and the friction between the fragments will lead to the release of heat in abundance, which contributes to the appearance of melting zones near the interface.

Colloidal Solutions

The internal structure of the localized-melting zones substantially depends on the mutual solubility of the constituent metals in the liquid state. As shown in [3, 5], in the case of titanium–aluminide joints, these zones are solid solutions of titanium alloyed with niobium and aluminum that were originally in the aluminide. Another situation arises if the original metals

do not have mutual solubility. In this case, these zones of localized melting are colloidal solutions, in which particles of the initial elements are mixed. Here, we only consider the case when no boiling of any of the materials occurs in explosive welding and, thus, the gas phase does not form. In this case, one should consider the possible forms of colloidal solutions [14]. The relationship between three temperatures is significant, i.e., $T_m^{(1)}$ is the melting point of the metal (1); $T_m^{(2)}$ is the melting point of metal (2); and T_b is the temperature near the interface.

Various relations are schematically shown in Fig. 10, assuming (for simplicity) that the $T_m^{(1)} > T_m^{(2)}$. Consider the case (Fig. 10a) when

$$T_m^{(1)} > T_b > T_m^{(2)}. \quad (1)$$

If condition (1) is valid, then a melt of the low-melting phase appears (hatching in Fig. 10a), which contains solid particles of the high-melting phase. This is a colloidal solution of the suspension type. Here, the absence of mutual solubility is of no concern and no separation occurs. The colloidal solution is mixed due to the circulation, which subsequently solidified into a suspension that was dispersion-strengthened by the particles of the high-melting phase. In this case, the zones of localized melting present no hazard to the joint stability; however, on the contrary, may contribute to its strengthening.

Consider the case (Fig. 10b) when

$$T_b > T_m^{(1)} > T_m^{(2)}. \quad (2)$$

This means that both of the metals are in molten states (double hatching in Fig. 10b) within the interval $T_b > T > T_m^{(1)}$. The strong external impact break both liquids into droplets, so a colloidal solution of the emulsion type forms. However, the emulsion is generally unstable. Droplets of the same type stick together, resulting in separation into two immiscible liquids. As in the case of so-called dilute emulsions (when the concentration of one phase is much smaller than the other), when the separation has no time to occur, the solidification of one element within the range of $T_m^{(2)} < T < T_m^{(1)}$ takes place and its droplets turn into solids, whereas the second element remains liquid. In the subsequent solidification, the colloidal solution becomes a solid dispersion-hardened suspension. In the alternative case (Fig. 10c), when

$$T_m^{(1)} > T_m^{(2)} > T_b, \quad (3)$$

neither metal melts and no colloidal solutions are formed.

Thus, in the case of colloidal solutions of immiscible liquids, an emulsion or suspension forms. In the solidification, the emulsion is a danger to the continuity of the joint due to the possible separation; conversely suspension can strengthen the joint.

The characteristic temperatures of the joints under study are approximately $T_m^{(Ta)} = 3300$ K, $T_m^{(Cu)} = 1300$ K; $T_m^{(Fe)} = 1800$ K, and $T_m^{(Ag)} = 1200$ K. If the assumption is made that the temperature near the interface is $T_b \approx 1500$ – 1700 K, then the relation (1) is valid for both joints and dispersion-strengthening suspension forms, which ensures their strength. If $T_b \approx 2000$ K, then the relation (2) is valid for both joints and an emulsion forms. As can be seen from Figs. 3, 4, an emulsion is heterogeneous in various regions. The emulsion is diluted where spherulites are observed (Fig. 4). However, the emulsion shown in the image in Fig. 3 is concentrated. These are regions where separation can appear. Here, however, no layers of iron were observed. This means that quenching is so fast that the separation has no time to occur.

Dendrites

It is known that dendritic growth [15] begins when the liquid phase has a negative temperature gradient. In this case, this is true because the region near the interface is the hottest. The melting occurs almost instantaneously under explosion, but dendrites grow at residual temperatures when diffusion becomes possible.

The coefficient of thermal conductivity of silver is about 418.7 W/(m K) and is one of the highest among metals. The thermal conductivity of iron is 74.4 W/(m K). The difference in the coefficients of thermal conductivity causes the heat to sink from the interface through the silver. As can be seen from Fig. 8a, the thickness of

the melted layer of silver is about 200 μm . Calculations for determining whether there is enough energy supplied to melt the desired silver band are given below. For this purpose, we use the following values of parameters for silver: an atomic weight of 107.9 , density of 10.5 g/cm³, melting temperature $T_m = 1234$ K, melting heat $Q_m = 11.34$ kJ/mol, and heat capacity $C_v \approx 24$ J/(mol K).

Hence, it is easy to show that the energy required to melt this layer E_m is approximately 0.23 MJ/m², and the energy required to heat it E_h to 1000 K is approximately 0.48 MJ/m². Thus, the total energy required to heat and melt a 200 - μm -thick silver layer is $E_t \approx 0.71$ MJ/m².

This estimate is too high, since the total energy injected during the explosion of the iron–silver system is only 0.73 MJ/m². However, here, the energy required to fragment and heat iron and silver away from the melting zone, etc. was not considered. However, it has also not been taken into account that the dendrite layer has a thickness of less than 200 μm in many places, which may reduce the energy required for melting. Thus, in general, we can assume that the energy balance is sufficient for heating and melting the silver layer.

CONCLUSIONS

(1) A structural study of the joints of metals without mutual solubility (copper–tantalum and iron–silver) resulted in a foundation in which, under explosive welding, the interpenetration of the materials is carried out by the formation of protrusions, the ejection of particles of one material into another, and the formation of zones of localized melting.

(2) Granulating fragmentation is observed. GF is the process of separation into particles, which either fly apart or merge with each other. The role of GF in explosive welding was understood to be one of the most efficient ways of dissipating the energy supplied. To a certain extent, GF is analogous to the fragmentation at the explosion, which was studied by Mott. GF results from microdestructions and is an alternative process to destruction.

(3) It was shown that, in the case of joints of metals with normal solubility, the localized-melting zones formed true solutions, whereas in the case of metal joints without mutual solubility, the localized-melting zones formed colloidal solutions.

(4) It was shown that the investigated joints could form either emulsions or dispersion-strengthened suspensions. When solidified, the emulsion presents a hazard to joint stability due to possible separation; conversely, suspension can contribute to the strengthening the joint. Thus, the risk areas that can arise in the absence of mutual solubility were identified. The results can be used to develop new metal joints without mutual solubility.

ACKNOWLEDGMENTS

Electron microscopic studies were performed at the Electron Microscopy Center of Collaborative Access, Urals Branch, Russian Academy of Sciences. This work was supported in part by the Russian Foundation for Basic Research, project no. 10-02-00354; by projects 12-2-006-UT, 12-U-2-1011, 12-2-2-007 of the Ural Branch of the Russian Academy of Sciences; and by the National Target Program of Ukraine “Nanotechnologies and Nanomaterials,” no. 1.1.1.3-4/10-D.

REFERENCES

1. A. A. Deribas, *Physics of Strengthening and Welding by Explosion* (Nauka, Novosibirsk, (1980) [in Russian].
2. V. I. Lysak and S. V. Kuzmin, *Explosion Welding* (Mashinostroenie, Moscow, 2005) [in Russian].
3. V. V. Rybin, I. I. Sidorov, B. A. Greenberg, O. V. Antonova, O. A. Elkina, A. V. Inozemtsev, A. M. Patselov, and M. A. Ivanov, “Formation of Vortices during Explosive Welding (Titanium–Orthorhombic Titanium Aluminide),” *Phys. Met. Metallogr.* **108**, 353–364 (2009).
4. V. V. Rybin, B. A. Greenberg, M. A. Ivanov, S. V. Kuz'min, V. I. Lysak, O. A. Elkina, A. M. Patselov, A. V. Inozemtsev, O. V. Antonova, and V. E. Kozhevnikov, “Structure of the Welding Zone between Titanium and Orthorhombic Titanium Aluminide for Explosion Welding: I. Interface,” *Russ. Metall. (Metally)* **2011** (10), 1008–1015 (2011).
5. B. A. Greenberg, M. A. Ivanov, V. V. Rybin, S. V. Kuz'min, V. I. Lysak, O. A. Elkina, A. M. Patselov, O. V. Antonova, and A. V. Inozemtsev, “Structure of the Welding Zone between Titanium and Orthorhombic Titanium Aluminide for Explosive Welding: II. Local Melting Zones,” *Russ. Metall. (Metally)* **2011** (10), 1016–1025 (2011).
6. V. V. Rybin, B. A. Greenberg, M. A. Ivanov, A. M. Patselov, O. B. Antonova, O. A. Elkina, A. V. Inozemtsev, and G. A. Salishchev, “Nanostructure of Vortex during Explosive Welding,” *J. Nanosci. Nanotechnol.* **11**, 8885–8895 (2011).
7. B. A. Greenberg, M. A. Ivanov, V. V. Rybin, O. A. Elkina, A. M. Patselov, O. B. Antonova, A. V. Inozemtsev, G. A. Salishchev, and V. E. Kozhevnikov, “Transition Zone Structure and Its Influence on the Strength of Copper–Tantalum Explosion Welded Joint,” *Deform. Razrush. Mater.*, No. 9, 34–40 (2011).
8. B. A. Greenberg, O. A. Elkina, O. V. Antonova, A. V. Inozemtsev, M. A. Ivanov, V. V. Rybin, and V. E. Kozhevnikov, “Peculiarities of Formation of Structure in the Transition Zone of Cu–Ta Joint Made by Explosion Welding,” *The Paton Welding J.*, No. 7, 20–25 (2011).
9. B. A. Greenberg, M. A. Ivanov, V. V. Rybin, A. V. Inozemtsev, O. V. Antonova, O. A. Elkina, A. M. Patselov, S. V. Kuzmin, V. I. Lysak, and V. E. Kozhevnikov, “Inhomogeneities of the Interface Produced by Explosive Welding,” *Phys. Met. Metallogr.* **113**, 176–189 (2012).
10. V. V. Rybin, *Large Plastic Deformations and Fracture of Materials* (Metallurgiya, Moscow, 1986) [in Russian].
11. L. I. Markashova, V. V. Arsenyuk, G. M. Grigorenko, and E. N. Berdnikova, “Peculiarities of Mass Transfer Processes at Different Metal Welding by Pressure,” *Svaroch. Proizvod.*, No. 4, 28–35 (2004).
12. R. Z. Valiev and I. V. Aleksandrov, *Bulk Nanostructural Metal Materials* (Akademkniga, Moscow, 2007) [in Russian].
13. N. F. Mott, “Fragmentation of Shell Cases,” *Proc. Roy. Soc. A* **189**, 300–308 (1947).
14. B. D. Summ, *Fundamentals of Colloid Chemistry* (Akademiy, Moscow, 2009) [in Russian].
15. M. Flemings, *Solidification Processing*, (New York: McGraw-Hill, 1974).